RPE | Radiation Physics & Engineering
A Peer-Reviewed Journal
Published by K.N. Toosi University of Technology
http://rpe.kntu.ac.ir
Research Article

Radiation Physics and Engineering 2024; 5(1):11–19

Benchmark MCNP computer code simulation results against experimental data of neutron flux and spectrum from neutron imaging system of Tehran research reactor

Majid Zamani, Mohsen Shayesteh*

Physics Department, Imam Hossein University, P.O. Box 16575-347, Tehran, Iran

HIGHLIGHTS

- Irradiation of samples by monochromatic neutron beam of E-beam tube.
- Using the neutron activation method to determine the neutron flux.
- Investigating the neutron imaging system of the Tehran Research Reactor (TRR).
- Unfolding the neutron energy spectrum.
- Benchmark study to validate the calculation tool against experimental data.

ABSTRACT

Using the experimental data in nuclear computing to verify the calculation methods and tools based on numerical and statistical methods has many benefits such as illustrating the quality, ensuring the capabilities, and validating computer codes. Simulation by computer tools is also applicable in the safety analysis of research reactors. In this research, the computer tool (MCNPX 2.7.0: 2011) was verified against the experimental data of neutron flux and spectrum on the sample position of the Tehran Research Reactor (TRR) neutron imaging system by the neutron activation method. To determine the benchmark specifications, the simulation of the system was done at the first step by considering a well-defined facility geometric, material specification and reactor core configuration, fuel elements, and radiation facility (beam tubes and collimator, reactor core, and neutron imaging components). Then the flux and neutron spectrum at the sample position were calculated. In the second step, a set of In (bare and covered by cd) and Au foils and a set of Au, Ni, Ti, and Zr, were placed and exposed almost in front of the reactor E beam tube. The neutron energy spectrum was unfolded by calculating the saturation activity of each foil by SAND-II code, and the neutron flux was calculated. A comparison of the results obtained in two steps shows a relatively good and acceptable agreement (Max. 30% deviation) between the flux and the shape of the flux profile obtained from calculations and experimental data.

KEYWORDS
Benchmarking
MCNPX
Neutron flux
Spectrum
Neutron imaging
Tehran Research Reactor

HISTORY
Received: 13 July 2023
Revised: 31 July 2023
Accepted: 16 August 2023
Published: Winter 2024

1 Introduction

Accompanying progress in computer technology and numerical methods, the capabilities of computer codes in the field of nuclear computing have been substantially enhanced. The recent development of these methods and tools allows for better simulation of the complex processes during the routine operation and transient conditions of research reactors (IAEA, 2022). Correct application of these methods and codes is an essential part of design improvement, operation, utilization, and safety aspects of research reactors and associated experiments. In many institutions operating these reactors, these codes are used daily for technical support of operation and analysis of parameters related to reactor safety.

However, the benchmarking process of computational codes and the use of available experimental data to verify or the calculation methods and tools which uses numerical-statistical methods, are always an important topic for conducting research (IAEA, 2022).

To demonstrate the quality of these computational methods and codes, it is important to benchmark them

*Corresponding author: mshayesteh@ihu.ac.ir

https://doi.org/10.22034/rpe.2023.406935.1152

Table 1: Summary of benchmarking calculations, using the foil activation in active research reactors.

Reactor	Country	Experiment name	Type of experiment	Benchmark contributors	Codes used
OPAL	Australia	ANSTO-2	Structure material activation	Argentina, Australia France	MCNP5, ORIGEN, MCNP6, DARWIN2, TRIPOLI- 4
		ANSTO-3	Activation of Au grains	Argentina, Australia, Slovenia	CONDOR, CITVAP, MCNP5, MCNP6
ATI	Austria	ATI-2	Foil activation	Austria, Slovenia	Serpent 2, MCNP6, FISPACT-II
ETRR-2	Egypt	EAEA-2	Cs-134/Cs-137 activity ratio in LEU targets	Australia, Egypt	AUS98, Analytical model, MCNPX v2.7
IPEN/ MB-01	Brazil	IPEN/ MB-01	Mo-99 activation	Argentina, Brazil, South Africa	MCNP5, SCALE, MCNP6, FISPACT-II, OSCAR-5
JSI TRIGA Mark II	Slovenia	JSI-1	Foil activation	Argentina, Slovenia	MCNP5, FISPACT-II, MCNP6
SAFARI-1	South Africa	NECSA-2	Be poison activation	Romania, South Africa	MCNPX v2.7, OSCAR-5/MGRAC, OSCAR-5

against experimental data as part of assessing the validity of their application to the design, operation, and safety analysis of research reactors, regarding in use of radiation applications such as neutron imaging. Therefore, benchmarking of calculation results against experimental data, such as the calculation of reactor fuel burnup rate (El Bakkari et al., 2009) or neutron activation of materials (Tiyapun et al., 2015; Di Tigliole et al., 2014), has significant benefits and applications in fields of evaluating the accuracy of calculations in the design, operation, and safety data analysis of the research reactors, including the Tehran research reactor (TRR).

To conduct the benchmarking of MCNP code or other nuclear codes (Iwamoto et al., 2017), through the neutron activation experiment and then the calculation of neutron spectrum and flux or through the other experiments (Olsher et al., 1993), it is sufficient to have the technical specifications of benchmarking. Technical specifications include the reactor descriptions and experimental data available in advance or being measured during an experiment (IAEA, 2022). The mentioned specifications have already been prepared for many important research reactors in advance and are used as a reference for conducting benchmarking tests (IAEA, 2015).

Table 1 shows the list of reactors for which the nuclear code verification test was performed through the neutron activation method. TRR is not in Table 1, so the purpose of the current research is to benchmark the used computer tool (MCNPX 2.7.0: 2011) results against the experimental data of only neutron flux and spectrum through the neutron activation of targets (as the technical specifications), for use in future applications in the TRR neutron imaging.

2 Material and Methods

The benchmarking test and analysis using the MCNP calculation method of the TRR core, components, and neutron imaging system elements require the technical specifications of benchmarking. This specification consists of two parts. The first is a complete geometric description of the reactor, such as dimensions, core layout, configuration, fuel elements, and radiation facility structure, including beam tubes and collimators, used for simulation and modeling of system components and code calculations. The second is the experimental data, which includes the results of measurements in a radiation facility through neutron activation of fixed foils in the sample position. The dimensions, weight, and materials of the irradiated sample, the duration of irradiation and the subsequent decay time to measure the saturated activity, and finally the neutron flux and spectrum calculations are also considered in this part.

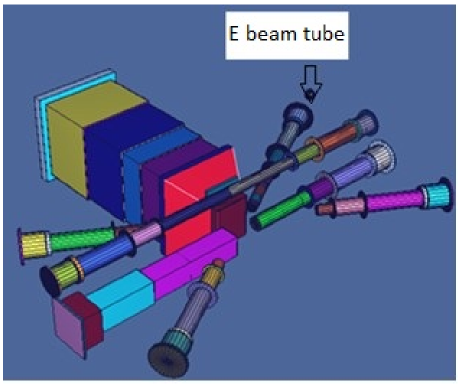

Figure 1: A 3D geometry of the TRR model. Beam tubes (A to H), thermal columns, and other structural components of the TRR are shown.

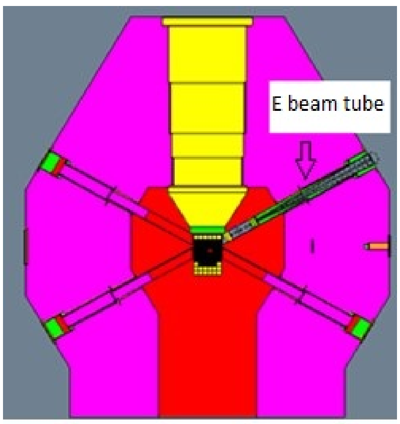

Figure 2: 2D view of MCNP model of the TRR North West beam tube (E) position.

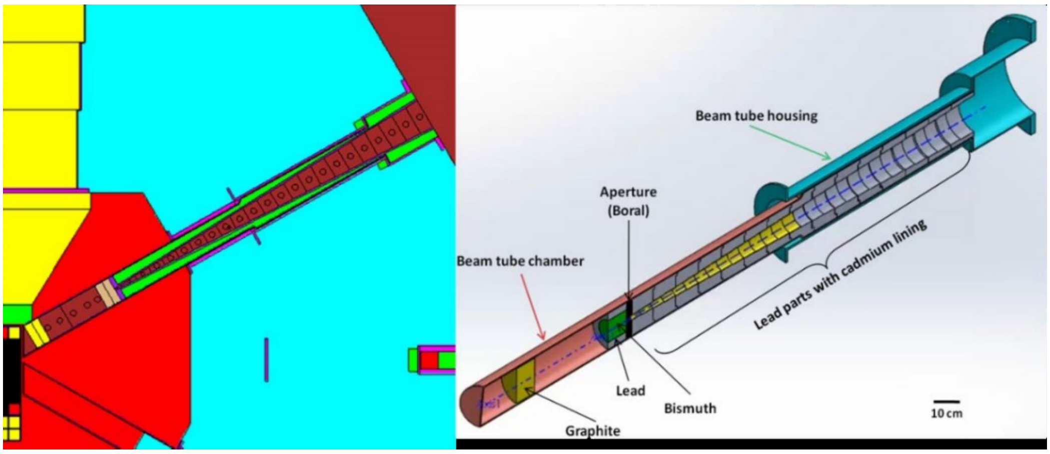

Figure 3: A view of the neutron collimator designed to be installed in the beam tube E.

2.1 Reactor's Technical Specifications

Tehran Research Reactor is a pool-type reactor with thermal power of 5 MW with Low Enrichment Uranium (LEU) plate fuel (20% U-235) and with light water as a coolant and reflector media. This reactor is used to produce radioisotopes, activate samples, and for educational purposes. This reactor is also equipped with auxiliary systems for the use of neutron beams and gamma rays produced in the core of the reactor in various research fields. This equipment includes radiation channels, thermal columns, etc. In addition, this reactor has seven beam tubes. The location of this equipment is shown in 3D in Fig. 1. An MCNP geometric simulation of the reactor core and components are also illustrated in 2D in Fig. 2.

To obtain a thermal neutron beam for neutron irradiation purposes, a neutron collimator has been designed and installed inside a 6-inch E-beam tube (Fig. 3), and has been successfully tested (Dastjerdi and Khalafi, 2015; Dastjerdi et al., 2017, 2016). Having neutron and gamma filters, this collimator can greatly reduce gamma rays and fast neutrons in addition to parallelizing neutrons from the reactor core and improving the quality of neutron images. Bipolycrystal has been used as a gamma filter and graphite as a filter for fast neutrons. Figure 4 shows the configuration of arrangement No. 7 of the medium TRR core.

The support plate consists of a 9×6 Aluminum grid with dimensions of 75×46 cm, which has 54 potential locations for the placement of fuel rods. Also, empty spaces are created for sample radiation in the core. This core contains 24 SFE and 5 CFE. Each SFE contains 19 fuel

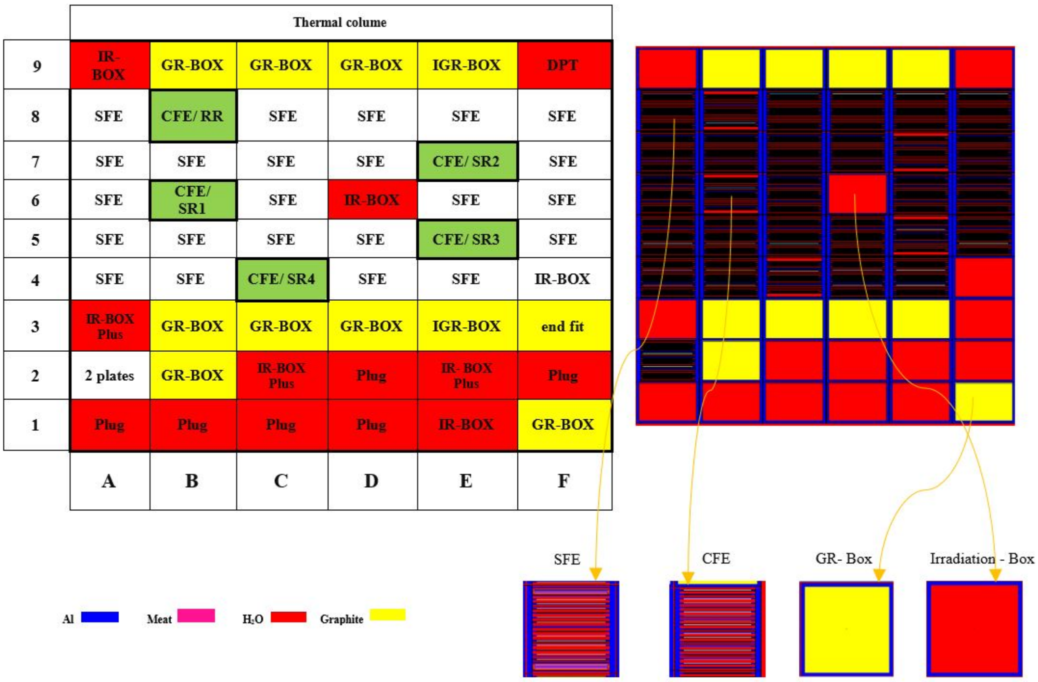

	Thermal colume					
9	IR-BOX	GR-BOX	GR-BOX	GR-BOX	IGR-BOX	DPT
8	SFE	CFE/ RR	SFE	SFE	SFE	SFE
7	SFE	SFE	SFE	SFE	CFE/ SR2	SFE
6	SFE	CFE/ SR1	SFE	IR-BOX	SFE	SFE
5	SFE	SFE	SFE	SFE	CFE/ SR3	SFE
4	SFE	SFE	CFE/ SR4	SFE	SFE	IR-BOX
3	IR-BOX Plus	GR-BOX	GR-BOX	GR-BOX	IGR-BOX	end fit
2	2 plates	GR-BOX	IR-BOX Plus	Plug	IR-BOX Plus	Plug
1	Plug	Plug	Plug	Plug	IR-BOX	GR-BOX
	A	B	C	D	E	F

Figure 4: Configuration of arrangement No. 7 of the TRR medium core (left side), Radial representation of the TRR core, and a partial view (Y-X modelling) of various types of SFE, CFE, and Graphite Box.

plates and each CFE contains 14 fuel plates with a enrichment of 19.7. Control rods are placed in these complexes (Dehkordi et al., 2019).

2.2 Neutron Radiography Room's Technical Specifications

A room equipped with the necessary equipment for digital neutron radiography (NR), including a shutter, sample table, beam catcher, and automation system for transfer and processing of recorded images, was built adjacent to the E-beam tube (Rokrok et al., 2021) and evaluated for neutron imaging quality (Kasesaz et al., 2020).

As seen in Figs. 5 and 6, there is a corridor outside the room and the exit door is at the end of this corridor. The walls are 55 cm thick and made of reinforced concrete. The structure and materials used in the beam catcher (Fig. 6) reduce the neutron and gamma dose rates to as low as reasonably possible levels (Dastjerdi et al., 2017). Due to technical reasons, the height of the part of the chamber ceiling, which is placed on top of the E tube beam, is 145 cm higher than the ceiling.

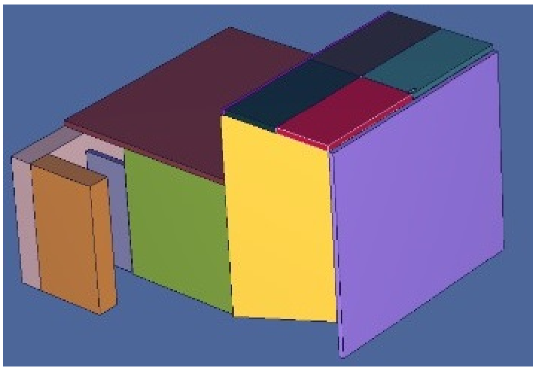

Figure 5: Final design: the designed room has a curved corridor outside the room and walls of the same thickness.

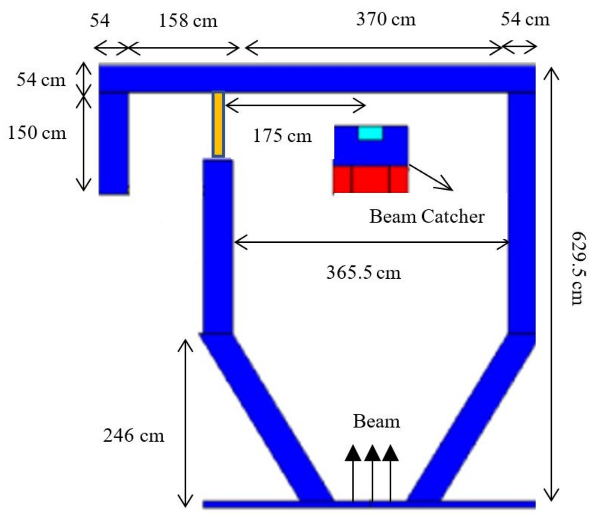

Figure 6: Design and installation of the new roof of the neutron imaging room of the Tehran reactor, 3D design (right side).

To reduce the total dose rate outside the room, the door was covered with two layers of borate polyethylene each 5 cm thick, and two layers of lead each 3 mm thick. Figure 7 shows its schematic design. The schematic design of the beam catcher is shown in Fig. 8. In this design, the thickness of the lead layer is 25 cm. The diameter of the beam catcher entrance is 50 cm, so according to the divergence angle of 2 degrees of the neutron beam, this equipment was placed at a distance of 450 cm from the E-beam tube.

2.3 Computer code and used libraries

MCNPX 2.7.0 computer code is used for simulation (Pelowitz et al., 2005). This code simulates the transport of particles such as neutrons, photons, and electrons using the Monte Carlo method. Due to the use of the Monte Carlo method, the results obtained from this code are always associated with statistical error or variance. In cases where the statistical error of calculations is high, different variance reduction methods can be used and better results can be obtained. In this research, to simulate the reactor core and its components, the source is defined as a circular disc with a diameter of 15 cm (equal to the cross-sectional area of the E-beam tube). Neutrons are emitted from this source isotropically in the form of a cone with a divergence angle of 2 degrees.

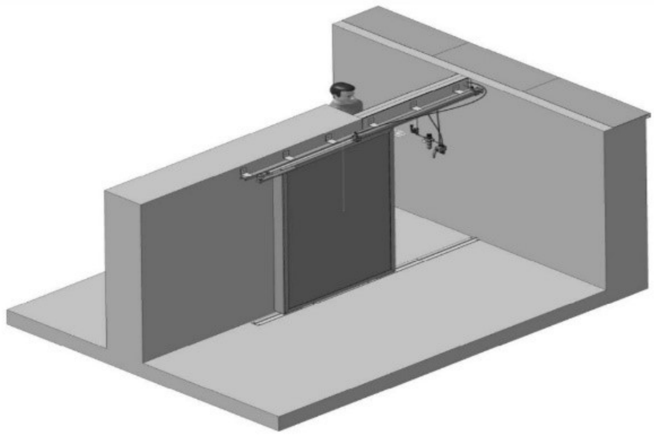

Figure 7: Neutron Radiography room and door plan.

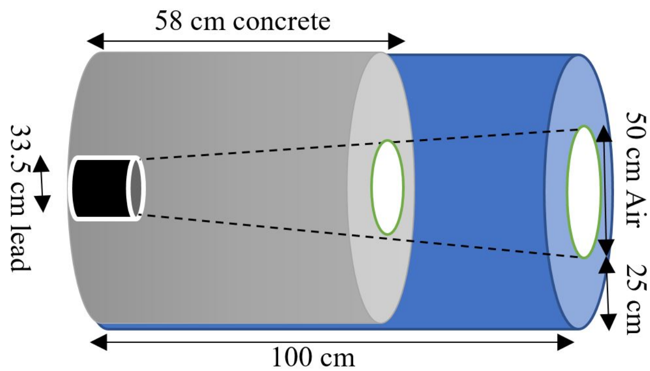

Figure 8: Schematic image of the beam catcher installed in the neutron radiation room.

Table 2: Characterization of the irradiated foils.

Sample code	Foil material	Foil mass in datasheet (g)	Measured mass (g)	Nuclear interaction	Energy threshold	Half-life (d)	Irradiation time (s)	Cooling time (s)
AE	In	0.13	0.1351	^{115}In(n,n')^{116}In^m	2.1-2.9 MeV	0.18691	9180	254
AC	In + Cd	0.13	0.1372	^{115}In(n,γ)^{116}In^m	Thermal	0.03761	9180	254
E	Ni	0.28	0.2817	^{58}Ni(n,p)^{58}Co	2.9 MeV	71.3	28800	151200
G	Ti	0.14	0.1435	^{46}Ti(n,p)^{46}Sc, ^{48}Ti(n,p)^{48}Sc	5.5 MeV, 2.1 MeV	83.3, 3.41	28800	151200
I	Zr	0.11	0.115	^{90}Zr(n,2n)^{89}Zr	12.3 MeV	3.2670	28800	151200
K	Au	0.12	0.1278	^{197}Au(n,γ)^{198}Au	Thermal	2.7	28800	151200

Table 3: The results of measured saturation activity and saturation activity calculated by SAND-II code (after 25 repetition limit).

Foil Reaction	Saturated Measured Activity (DPS/Nucleus)	Saturated Calculated Activity (DPS/Nucleus)	Normal 5.00 Percent Activity Limits (MeV)		Ratio Measured to Calculated Activities	Deviation of Measured from Calculated Activity
			Lower	Upper		
^{197}Au(n,γ)^{198}Au	5.63E-16	5.18E-16	1.50E-08	2.55E-01	1.0872	8.72%
^{197}Au(n,γ)^{198}Au Cd	5.25E-17	5.36E-17	4.00E-04	5.25E-01	0.979	-2.1%
^{115}In(n,γ)^{116m}In	7.54E-16	8.18E-16	1.60E-08	2.80E-07	0.9219	-7.81%
^{115}In(n,γ)^{116}In^m	4.11E-17	4.03E-17	1.50E-03	6.00E-01	1.0205	2.05%
^{46}Ti(n,p)^{46}Sc	2.81E-19	2.68E-19	5.00E+00	1.24E+01	1.0498	4.98%
^{48}Ti(n,p)^{48}Sc	2.41E-20	2.48E-20	7.20E+00	1.35E+01	0.9703	-2.97%
^{115}In(n,n$'$)^{115m}In	1.09E-18	1.11E-18	4.00E-01	9.30E+00	0.9838	-1.62%
^{115}In(n,n$'$)^{m}Cd	1.08E-18	1.09E-18	4.25E-01	9.30E+00	0.9875	-1.25%

To calculate the neutron flux and spectrum at the sample location (in front of the E-beam tube and 100 cm from the outlet), Tally F4 and ENDF/B-VII.0 nuclear data library (Chadwick et al., 2006) were used. For calculations of the neutron flux, triple binding energy consisting of thermal, epithermal, and fast neutrons in the range of up to 2.5×10^{-8}, 1×10^{-2}, and 20 MeV, respectively was selected. For calculations of the neutron spectrum in multigroup mode and to include the lowest possible energy interval, the energy division was done in 618 groups. DXTRAN spheres are used as a variance reduction technique, a combination of two variance reduction techniques, Russian roulette, and non-analog probability density function sampling. The DXTRAN spheres (with inner and outer radiuses of 11 and 12 cm, respectively) are placed exactly around the location of the samples, at a distance of 100 cm from the E-beam tube.

2.4 Experimental data

The method used in this research to measure thermal neutron flux and non-thermal neutron flux (epithermal and fast) at the sample location is neutron activation of two types of metal foils. The estimation of the minimum time required for irradiating the samples was carried out by considering the minimum activity required for detection by the laboratory detector system, which is a High-Purity Germanium Detector (HPGe), and the technical characteristics of the samples based on equation Eq. (1)

$$A = N\varphi\sigma(1-\mathrm{e}^{-\lambda t_a})\mathrm{e}^{-\lambda t_w} \qquad (1)$$

where t_a and t_w are the irradiation time and the time interval between the end of irradiation and the start of counting, respectively, is the number of target atoms, is the absorption cross-section of target nuclei, is the decay constant of activation products, is the activity of interaction products in neutron activation and is the thermal neutrons flux. Based on these estimations, short-term irradiation (9180 s) of In foils with and without Cd cover with a cooling time of 254 s and long-term irradiation (28800 s) of Ti, Ni, Zr, In, and Au foils with a cooling time of 151200 s were done. Foils specification data used in irradiation conditions are given in Table 2. Standard irradiated circular samples are 0.5 inches (1.27 cm) in diameter and all 0.02 inches (0.0508 cm) thick.

After the samples were irradiated and cooled down in the laboratory, to calculate the specific activity of the irradiated samples, gamma rays were counted using an HPGe detector, and the neutron flux was unfolded in the different energy bins based on neutron activation reactions and the results of the SAND-II code output (SNL-SANDII, 1996).

This code works based on the repetition algorithm. By entering the saturation activity of each foil, the initial guess of the neutron energy spectrum (Fig. 9) (Zamani and Shayesteh, 2022), appropriate correction, and weighting coefficients as inputs, the estimated neutron spectrum is extracted in each execution cycle and close to the real spectrum. This code does not define the geometry of the neutron source, foils, and their radiation test environment. Meanwhile, these factors are influential in the results of measuring the activity of foils (Heydarzade et al., 2018).

The results of measured saturation activity, calculated saturation activity, and deviations (all less than 10%) in the output of the SAND-II code execution are presented in Table 3.

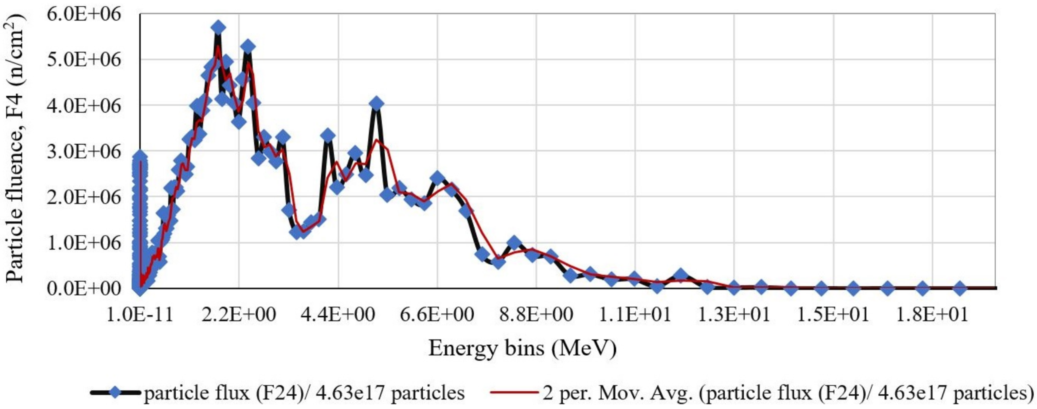

Figure 9: Neutron spectrum in different range of energies (thermal, epithermal and fast), in front of E beam tube.

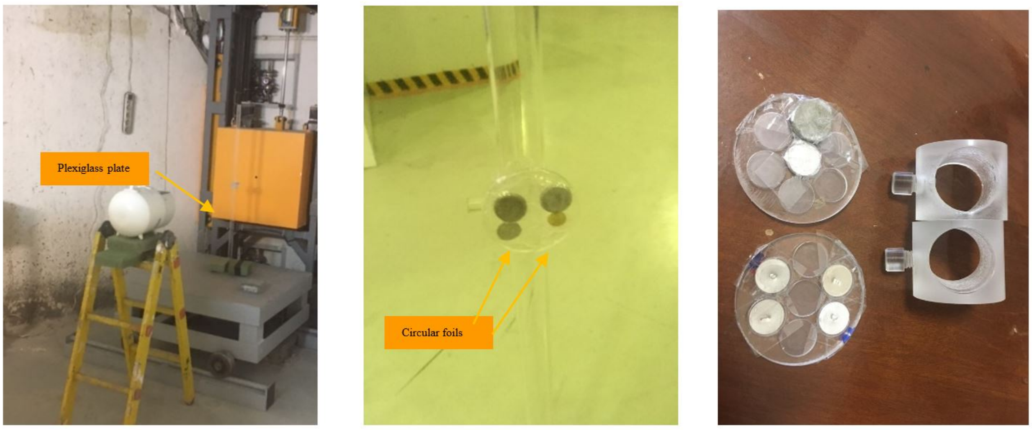

Figure 10: The connecting piece of the samples to the base (right), Installing the samples on the plexiglass plate and connecting it to the base (middle), placing the base and the plate holding the samples in front of the beam tube E (left).

The results obtained from the SAND II code show a good agreement between the results of this code and the measured values. Figure 10 shows a view of how to install and connect the first and second sample foils on the plate and support base (transparent plexiglass) and its placement in the sample location in the neutron imaging laboratory.

3 Results and Discussion

By comparing the results of experimental measurements and calculations, the code can be benchmarked to obtain a degree of consistency between the results. A comparison of calculated and measured non-thermal and thermal neutron spectra is given in Figs. 11 and 12, respectively. Each Figure has 2 diagrams including a moving average line trending diagram for each graph. The comparison of measured and calculated neutron flux is given in Table 4.

The results obtained in this study show that in the neutron imaging system of the Tehran Research Reactor, the flux and spectrum calculated by the MCNP code are consistent with the experimental results of the saturation activity measurement. The deviation between the calculated and measured neutron flux and spectrum in the thermal neutron energy range (used in neutron imaging) is about 30%. This could be due to more scattering of low-energy neutrons from the walls and other elements in the neutron radiography room, while there is a greater agreement between the results in the epithermal and fast neutron energy range. These results show that the materials and geometric features used in the simulation are well modeled by the MCNP code in the imaging application. When comparing calculated results with experimental data, the variance of results and errors in simulation and measurement should be considered. However, most of the variances in the measurement results seem to be due to the position of the measurement point in three-dimensional space. Other causes of the difference between the results are temperature effects and uncertainties in the reactor power calibration, which directly affect the calculations. The proximity of the foils to each other and the effect of the activation plexiglass holding them on the laboratory count can also affect the final measurement results. On the other hand, the density of the material may not be equal to the actual values. In general, any slight differences in the geometry and materials used in the simulation with real conditions will cause differences between the measured values and the simulation results. In addition, the results of Tally F4 calculations in small and thin volumes (such as irradiated foils) are not very accurate. Also,

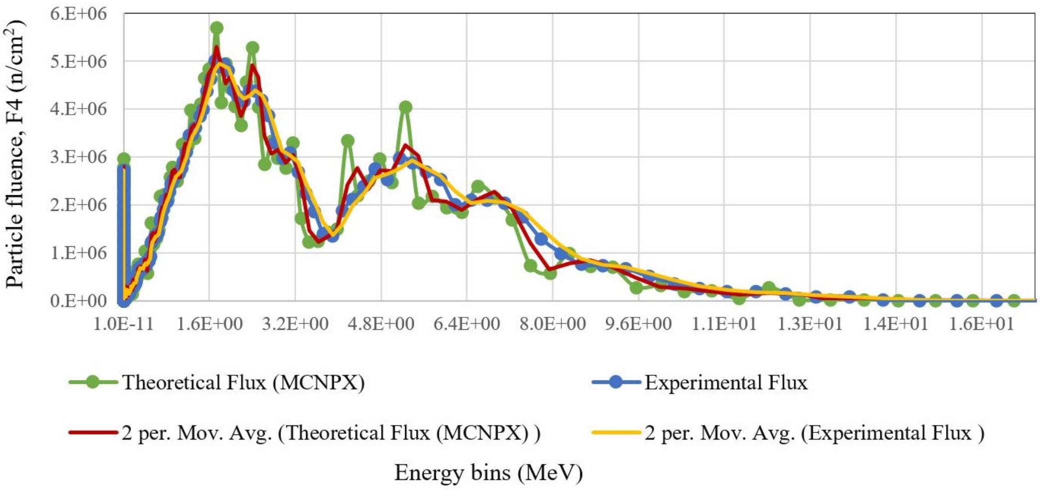

Figure 11: Comparison of neutron flux by MCNP (diagram with green circles) with the measurement in the laboratory (diagram with blue circles) in three energy ranges of thermal, epithermal, and fast neutrons - trending diagram of each graph, is indicated by continuous red and yellow graphs, respectively.

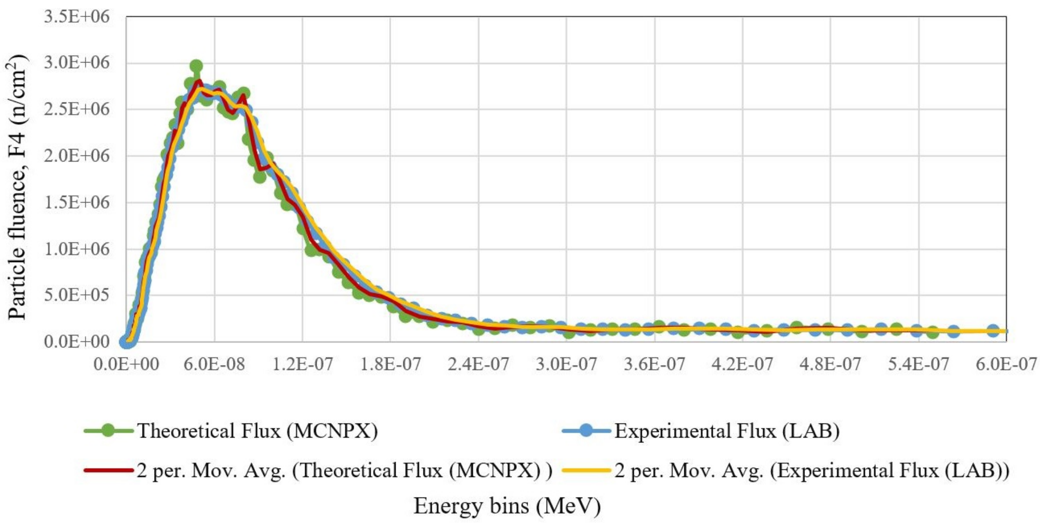

Figure 12: Comparison of the neutron flux by MCNP code (diagram with green circles) with the experimental results (diagram with blue circles) in thermal neutrons energy group, trending diagram related to the calculation and experimental results are marked with continuous red and yellow cycles, respectively.

Table 4: Comparison of calculated and measured neutron flux results in different neutron energy ranges.

Energy Group (MeV)	Calculated neutron flux by F4 Tally ($n.cm^{-2}.s^{-1}$)	Measured neutron flux in LAB ($n.cm^{-2}.s^{-1}$)	Deviation (%)
Thermal Neutrons (0- 2.5E-8 MeV)	5.33E+6	4.122E+6	29.36
Epithermal Neutrons (2.5E-8 - 0.1 MeV)	4.19E+5	3.754E+5	11.73
Fast Neutrons (0.1 - 20 MeV)	4.09E+6	3.955E+6	3.54

the neutron flux spectrum defined in the source card of the simulation program may not be completely accurate. In some cases, the saturation activity measurements of some radioisotopes may not fully match the simulation results. The reason for this could be that the gamma spectrum lines for measuring those isotopes are in the low energy region, where the uncertainty of the detector used is high and the measurement accuracy is lower.

There may be a discrepancy between the neutron spectrum taken as an initial input spectrum to start the SAND-II code run (to calculate the flux) and the input data provided. In addition to the above, the lack of cross-section in the library of this code for some materials used as a composite structure in the construction of the collimator and some other reasons cause the calculated neutron flux and spectrum to not fully match the experimental results. The results of the present research on neutron flux distribution can be used for future calculations such as spectrum calculations, dose rate calculations, various interaction rate calculations, reactor power selection factors, and reactor core kinetic parameter calculations.

4 Conclusions

The radiation system of the Tehran Research Reactor with the new changes made in it was simulated with the MCNPX code. In this research, the foil activation method was used to investigate the imaging system of the reactor. The activity of the samples was determined using an HPGe detector and the SAND-II code. The measured saturation activity and the calculated saturation activity for all eight samples used in this research are in good agreement with each other and their difference is less than 9% for all samples.

The neutron flux at the output of the E beam tube for three energy groups was calculated from Tally F4 of the MCNPX code, and the DXTRAN sphere was used to reduce the variance. The results obtained from these calculations are in acceptable agreement with the measured values of the flux obtained by the neutron activation method and using the SAND-II code to unfold the flux. This correspondence is about 30% for thermal neutrons and 12% and 3.5% for epithermal and fast neutrons, respectively.

Conflict of Interest

The authors declare no potential conflict of interest regarding the publication of this work.

References

Chadwick, M., Obložinskỳ, P., Herman, M., et al. (2006). ENDF/B-VII. 0: next generation evaluated nuclear data library for nuclear science and technology. *Nuclear Data Sheets*, 107(12):2931–3060.

Dastjerdi, M. C., Khalafi, H., Kasesaz, Y., et al. (2016). Design, construction and characterization of a new neutron beam for neutron radiography at the Tehran Research Reactor. *Nuclear Instruments and Methods in Physics Research Section A: Accelerators, Spectrometers, Detectors and Associated Equipment*, 818:1–8.

Dastjerdi, M. C., Movafeghi, A., Khalafi, H., et al. (2017). The quality assessment of radial and tangential neutron radiography beamlines of TRR. *Journal of Instrumentation*, 12(07):P07008.

Dastjerdi, M. H. C. and Khalafi, H. (2015). Design of a thermal neutron beam for a new neutron imaging facility at Tehran research reactor. *Physics Procedia*, 69:92–95.

Dehkordi, A., Habashi, S., and Rahimian, H. (2019). Neutronic and safety study of the dry channel in the Tehran Research Reactor core. *Proceeding of 26th Iran National Nuclear Conference.*

Di Tigliole, A. B., Cammi, A., Chiesa, D., et al. (2014). TRIGA reactor absolute neutron flux measurement using activated isotopes. *Progress in Nuclear Energy*, 70:249–255.

El Bakkari, B., El Bardouni, T., Merroun, O., et al. (2009). Development of an MCNP-tally based burnup code and validation through PWR benchmark exercises. *Annals of Nuclear Energy*, 36(5):626–633.

Heydarzade, A., Kasesaz, Y., and Mohammadi, S. (2018). Coupling the SAND-II and MCNPX codes for neutron spectrum unfolding. *Journal of Instrumentation*, 13(08):P08010.

IAEA (2015). Research Reactor Benchmarking Database: Facility Specification and Experimental Data, Technical Reports Series No. 480. *International Atomic Energy Agency.*

IAEA (2022). Benchmarks of Fuel Burnup and Material Activation Computational Tools Against Experimental Data for Research Reactors, Results of a Coordinated Research Project, TECDOC-1992. *International Atomic Energy Agency.*

Iwamoto, Y., Sato, T., Hashimoto, S., et al. (2017). Benchmark study of the recent version of the PHITS code. *Journal of Nuclear Science and Technology*, 54(5):617–635.

Kasesaz, Y., Rokrok, B., and C Dastjerdi, H. (2020). Radiation Safety Assessment of the New Neutron Radiography System at Tehran Research Reactor. *Radiation Safety and Measurement*, 9(4):251–256.

Olsher, R. H., Hsu, H.-H., and Harvey, W. F. (1993). Benchmarking the MCNP Monte Carlo code with a photon skyshine experiment. *Nuclear Science and Engineering*, 114(3):219–227.

Pelowitz, D. B. et al. (2005). MCNPX user's manual version 2.5. 0. *Los Alamos National Laboratory*, 76:473.

Rokrok, B., Choopan Dastjerdi, M. H., and Movafeghi, A. (2021). Design and construction of the neutron radiography facility for Tehran Research Reactor with real-time digital imaging capability. *NDT Technology*, 2(7):24–32.

SNL-SANDII (1996). Neutron Flux Spectra from Multiple Foil Activation Analysis. *Sandia national laboratories, Albuquerque, New Mexico, USA.*

Tiyapun, K., Chimtin, M., Munsorn, S., et al. (2015). Validation of the MCNP computational model for neutron flux distribution with the neutron activation analysis measurement. In *Journal of Physics: Conference Series*, volume 611, page 012007. IOP Publishing.

Zamani, M. and Shayesteh, M. (2022). Updated Calculation of Neutron and Gamma flux and Spectrum in E Beam Tube of Tehran Research Reactor, Used in Digital Neutron Imaging System. *Proceeding of 29th Iran National Nuclear Conference.*

To cite this article:

Zamani, M., Shayesteh, M. (2024). Benchmark MCNP computer code simulation results against experimental data of neutron flux and spectrum from neutron imaging system of Tehran research reactor. *Radiation Physics and Engineering*, 5(1), 11-19.

DOI: 10.22034/rpe.2023.406935.1152

To link to this article: `https://doi.org/10.22034/rpe.2023.406935.1152`